Bulletin of Earthquake Engineering (2020) 18:109–138
https://doi.org/10.1007/s10518-019-00721-1

ORIGINAL RESEARCH

Comparative analysis of liquefaction susceptibility assessment methods based on the investigation on a pilot site in the greater Lisbon area

Cristiana Ferreira[1] · António Viana da Fonseca[1] · Catarina Ramos[1] · Ana Sofia Saldanha[2] · Sara Amoroso[3,4] · Carlos Rodrigues[5]

Received: 25 January 2019 / Accepted: 16 September 2019 / Published online: 23 September 2019

Abstract

In Portugal, particularly in the greater Lisbon area, there are widespread alluvial sandy deposits, which need to be carefully assessed in terms of liquefaction susceptibility and risk zonation. For this purpose, a pilot site has been set up, as part of the European H2020 LIQUEFACT project. An extensive database of geological and geotechnical reports was collected and a comprehensive site investigation campaign was carried out, including boreholes with standard penetration (SPT), piezocone penetrometer and seismic dilatometer tests as well as geophysical methods, complemented by undisturbed soil sampling for laboratory characterisation. The assessment of liquefaction susceptibility based on field tests was made using the simplified procedure, considering the factor of safety against liquefaction (FS_{liq}), which relates the cyclic resistance ratio (CRR) with the cyclic stress ratio (CSR). While the computation of the CSR is relatively straightforward, the reliability of the CRR strongly depends on the adopted in situ testing technique. Alternative approaches to liquefaction assessment have been proposed, based on quantitative liquefaction damage indexes, namely the Liquefaction Potential Index (LPI) and Liquefaction Severity Number. In this paper, the geotechnical field data is integrated in these distinct approaches to liquefaction assessment. A comparative and in-depth analysis of the conventional approach is presented and the inclusion of specific information on soil type, as a means to overcome the observed differences, is discussed particularly for SPT and V_S results. The combination of these criteria enabled to clearly identify the most critical layers, in terms of liquefaction potential and severity.

Keywords Earthquake-induced liquefaction · Liquefaction potential · Site characterisation · In situ tests · Lisbon earthquake

List of symbols

a_g	Design ground acceleration on type A ground
a_{gR}	Reference peak ground acceleration on type A ground
a_{max}	Peak ground acceleration

✉ Cristiana Ferreira
cristiana@fe.up.pt

Extended author information available on the last page of the article

CH	Cross-hole test
CPTu	Piezocone penetrometer test
CRR	Cyclic resistance ratio
CSR	Cyclic stress ratio
C_σ	Overburden coefficient
DMT	Flat dilatometer test
DWF	Distance Weighting Factor
EC8	Eurocode 8
EC8-NA	Eurocode 8, National Annex
EILDs	Earthquake Induced Liquefaction Disasters
FC	Fines content
FS_{liq}	Factor of safety against liquefaction
g	Acceleration of gravity
h_{liq}	Height of liquefiable layer
I_C	Soil behaviour type index
I_D	Material index
K_{a1}	Ageing correction factor
K_{a2}	Ageing correction factor
K_D	Horizontal stress index from DMT
K_σ	Effective overburden stress coefficient
LPI	Liquefaction Potential Index
LSN	Liquefaction Severity Number
MSF	Magnitude scaling factor
MSF_{max}	Upper limit of MSF
M_w	Moment magnitude
$(N_1)_{60cs}$	Normalised equivalent clean sand SPT blow count number
p_a	Reference atmospheric pressure
PI	Plasticity index
P_L	Liquefaction probability
q_c	Cone tip resistance
q_{c1Ncs}	Normalised equivalent clean sand CPT cone tip resistance
Q_{cn}	Normalised cone tip penetration resistance
r_d	Shear stress reduction coefficient
S	Soil factor defined in EN 1998-1:2004
SASW	Spectral analysis of surface waves test
SCPTu	Seismic piezocone penetration test
SDMT	Seismic dilatometer test
SI	Site investigation point
S_{max}	Soil factor depending on ground type
SPT	Standard penetration test
SR	Seismic refraction test
u_2	Pore pressure
V_S	Shear wave velocity
V_S_AS	Shear wave velocity calculated with Andrus and Stokoe (2000)
V_S_KAE	Shear wave velocity calculated with Kayen et al. (2013)
V_{S1}	Stress-corrected shear wave velocity
V_{S1}*	Upper boundary value of V_{S1}
z	Depth
α	Parameter to calculate r_d

β	Parameter to calculate r_d
γ_I	Importance factor
σ'_v	Effective overburden stress
σ'_{v0}	Initial effective overburden stress
τ_{cyc}	Cyclic shear stress

1 Background on liquefaction assessment methods

Different approaches to the assessment of the liquefaction potential have been proposed. The most common approach is the "Simplified Procedure", originally proposed by Seed and Idriss (1971), which is also recommended by Eurocode 8 or EC8 (CEN 2010). According to this procedure, the factor of safety against liquefaction is computed from the ratio between the cyclic resistance ratio (CRR) and the cyclic stress ratio (CSR), as in Eq. 1. The CRR refers to the resisting capacity of the soil to liquefy, while the CSR corresponds to the design seismic action at a specific location in depth.

$$FS_{liq} = \frac{CRR}{CSR} \tag{1}$$

The liquefaction analysis framework proposed by Boulanger and Idriss (2014) was adopted, which is based on the simplified procedure proposed by Seed and Idriss (1971) and uses the parameters from previous works, namely r_d from Idriss (1999), K_σ from Idriss and Boulanger (2004, 2010) and the implementation of the fines content estimates from CPT (Idriss and Boulanger 2004, 2010). In this approach, the resistance values from SPT and CPTu are adjusted to incorporate the effect of fines content. Table 1 presents a summary of the expressions for computation of the governing parameters used in this analysis, as well as the respective references, to obtain the normalized CSR and the respective adjustment parameters.

On the other hand, the cyclic resistance ratio (CRR) can be estimated from lab and in situ test results. The standard penetration tests (SPT) and cone penetration test (CPT) are particularly convenient, given the extensive worldwide database and past experience. Moreover,

Table 1 Calculation of CSR and adjustment parameters adopted in the present work

Expressions for computation of the parameters	References
$CSR = \frac{\tau_{cyc}}{\sigma'_{v0}} = 0.65 \cdot \frac{a\max}{g} \cdot \frac{\sigma_{v0}}{\sigma'_{v0}} \cdot r_d$	Seed and Idriss (1971)
$r_d = e^{[\alpha(z)+\beta(z)\cdot M_w]}$	Idriss (1999)
$\alpha(z) = -1.012 - 1.126 \sin\left(\frac{z}{11.73} + 5.133\right)$	
$\beta(z) = 0.106 + 0.118 \sin\left(\frac{z}{11.28} + 5.142\right)$	
$CSR_{M=7.5,\sigma'_v=1atm} = \frac{CSR_{M,\sigma'_v}}{MSF \cdot K_\sigma}$	Idriss and Boulanger (2004, 2010)
$K_\sigma = 1 - C_\sigma \cdot \ln\left(\frac{\sigma'_v}{P_a}\right) \leq 1.1$	Idriss and Boulanger (2004, 2010)
$C_\sigma = \frac{1}{18.9-2.55\sqrt{(N_1)_{60cs}}} \leq 0.3$ or $C_\sigma = \frac{1}{37.3-8.27(q_{c1Ncs})^{0.264}} \leq 0.3$	
$MSF = 1 + (MSF_{max} - 1)\left[8.64exp\left(\frac{-M}{4}\right) - 1.325\right]$	Boulanger and Idriss (2014)
$MSF_{max} = 1.09 + \left(\frac{q_{c1Ncs}}{180}\right)^3 \leq 2.2$	

the use of the flat dilatometer test (DMT) has been developed in the last two decades, stimulated by the recognised sensitivity of the horizontal stress index K_D to a number of factors which are known to increase liquefaction resistance (difficult to sense by other tests), such as stress history, prestraining/aging, cementation, structure, and by its correlation with relative density and state parameter (Monaco et al. 2005). Shear wave velocities also provide a reliable assessment of liquefaction resistance of soils, since both depend on similar factors, namely confining stresses, soil type, void ratio and relative density (Andrus et al. 2004).

In this work, the proposals of Boulanger and Idriss (2014) based on SPT and CPT have been adopted (Eqs. 2 and 3), where $(N_1)_{60cs}$ and q_{c1Ncs} correspond to normalised equivalent clean sand values, as suggested by Idriss and Boulanger (2004, 2010). According to these authors, a clean sand is considered to have a fines content (FC) below 5%. It should be noted that the introduction of the FC in these approaches reflects its importance in the liquefaction susceptibility of the soil. However, the estimate of FC based on SPT tests can be ambiguous and may lead to inaccurate results of CRR especially for FC below 25%. Based on Idriss and Boulanger (2004, 2010), a correspondence between soil type and FC has been established, as detailed below (Sect. 4.1).

$$CRR_{7.5} = \exp\left(\frac{(N_1)_{60cs}}{14.1} + \left(\frac{(N_1)_{60cs}}{126}\right)^2 - \left(\frac{(N_1)_{60cs}}{23.6}\right)^3 + \left(\frac{(N_1)_{60cs}}{25.4}\right)^4 - 2.8\right) \quad (2)$$

$$CRR_{7.5} = \exp\left(\frac{q_{c1Ncs}}{113} + \left(\frac{q_{c1Ncs}}{1000}\right)^2 - \left(\frac{q_{c1Ncs}}{140}\right)^3 + \left(\frac{q_{c1Ncs}}{137}\right)^4 - 2.8\right) \quad (3)$$

For DMT-based liquefaction analyses, the Marchetti (2016) CRR-K_D curve has been used. Since the effects of higher fines content have not yet been fully investigated and clearly established, all the DMT triggering curves apply to clean sands. Therefore, the CRR is defined by combining the Idriss and Boulanger (2006) CRR-Q_{cn} correlation and the Robertson (2012) average Q_{cn}-K_D interrelationship (Eq. 4), where Q_{cn} is the normalized cone resistance. A combined correlation for estimating CRR based on Q_{cn} and K_D (Eq. 5) was also obtained by Marchetti (2016), by adopting the geometric average between a first CRR estimate obtained from Q_{cn} (Eq. 4) and a second CRR estimate obtained from K_D (introducing K_D into Eq. 4).

$$CRR_{7.5} = \exp\left(\frac{Q_{cn}}{540} + \left(\frac{Q_{cn}}{67}\right)^2 - \left(\frac{Q_{cn}}{80}\right)^3 + \left(\frac{Q_{cn}}{114}\right)^4 - 3\right), \text{ where } Q_{cn} = 25 \cdot K_D \quad (4)$$

$$\text{Average CRR} = \left[\left(\text{CRR from } Q_{cn}\right) \cdot \left(\text{CRR from } K_D\right)\right]^{0.5} \quad (5)$$

For the assessment of liquefaction resistance of soils based on shear wave velocities, two methodologies have been adopted, namely those proposed by Andrus and Stokoe (2000) and Kayen et al. (2013). Andrus and Stokoe (2000) follow the same approach of the simplified procedure, with CRR computed from the stress-corrected shear wave velocity in depth (V_{S1}), as follows:

$$CRR = \left[0.022 \cdot \left(\frac{K_{a1}V_{S1}}{100}\right)^2 + 2.8 \cdot \left(\frac{1}{V_{S1}^* - K_{a1}V_{S1}} - \frac{1}{V_{S1}^*}\right)\right] \cdot K_{a2}, \text{ where } V_{S1} = V_S \cdot \left(\frac{p_a}{\sigma'_{v0}}\right)^{0.25} \quad (6)$$

where V_{S1} is the normalised shear-wave velocity; K_{a1} and K_{a2} are ageing correction factors on V_{S1} and CRR, respectively, both corresponding to 1 for uncemented recent soils; V^*_{S1} is the upper boundary value of V_{S1} for liquefaction occurrence; p_a is the reference atmospheric pressure (= 100 kPa) and σ'_{v0} is the initial effective overburden stress.

On the other hand, Kayen et al. (2013) developed probabilistic correlations, based on a vast database of well-documented case histories, for V_S-based probabilistic and deterministic assessment of liquefaction susceptibility. In this paper, the deterministic approach has been employed for a liquefaction probability (P_L) of 15%, using the equations provided below. The respective factors of safety are computed, as before, as the ratio of the soil capacity to resist liquefaction at P_L (15%) and the corresponding seismic demand, CSR.

$$P_L = \Phi\left\{-\frac{[(0.0073 \cdot V_{s1})^{2.8011} - 1.946 \cdot \ln(\mathrm{CSR}) - 2.6168 \cdot \ln(M_w) - 0.0099 \cdot \ln(\sigma'_{v0}) + 0.0028 \cdot (\mathrm{FC})]}{0.4809}\right\}$$

$$\mathrm{CRR} = \exp\left\{\frac{[(0.0073 \cdot V_{s1})^{2.8011} - 2.6168 \cdot \ln(M_w) - 0.0099 \cdot \ln(\sigma'_{v0}) + 0.0028 \cdot \mathrm{FC} - 0.4809 \cdot \Phi^{-1}(P_L)]}{1.946}\right\} \tag{7}$$

Alternative approaches to the assessment of liquefaction potential have been suggested, mainly focusing on estimates of liquefaction-induced damages, based on quantitative liquefaction risk indexes, namely the Liquefaction Potential Index (LPI) and the Liquefaction Severity Number (LSN). Originally developed by Iwasaki et al. (1978), LPI combines the safety factor with depth, z, down to 20 m. Iwasaki et al. (1982) classification was adopted, as indicated in Table 2, since it is also implemented in CLiq® and the differences with other classifications are minor. The adopted colour code relative to each LPI class is also included in the table.

Tonkin & Taylor (2013) developed another quantitative indicator of the liquefaction-induced damages, the Liquefaction Severity Number (LSN). This index represents the expected damage effects of shallow liquefaction on direct foundations, based on post-liquefaction volumetric deformations, associated with reconsolidation settlements. Using this approach, the liquefaction severity can be classified in terms of expected damage, according to Tonkin & Taylor (2013), as in Table 3, where the adopted colour scheme is also shown.

2 Selection of the pilot site

2.1 Seismicity and liquefaction zonation of Portugal

Portugal's mainland and its Atlantic coast are located on the western and southern margins of the Iberian Peninsula. The seismicity of the Portuguese territory is heterogeneous and is classified according to regions with distinct seismic behaviour. Seismicity increases in

Table 2 Classification of liquefaction potential based on LPI (after Iwasaki et al. 1982)

LPI		Liquefaction potential
0	□	Very low
0 < LPI < 5	■ (green)	Low
5 < LPI < 15	■ (yellow)	High
15 > LPI	■ (red)	Very high

Table 3 Liquefaction severity and damage based on LSN (Tonkin & Taylor 2013)

LSN range	Typical performance
0 – 10	Little to no expression of liquefaction
10 – 20	Minor expression of liquefaction, some sand boils
20 – 30	Moderate expression of liquefaction, sand boils and some structural damage
30 – 40	Moderate to severe liquefaction, settlement can cause structural damage
40 – 50	Major expression of liquefaction, damage ground surface, severe total and differential settlements
> 50	Severe damage, extensive evidence of liquefaction, severe total and differential settlements affecting structures, damage to services

intensity from North to South, with a spatial distribution concentrated in the South and the Atlantic margins. According to existing records, earthquake epicentres are concentrated near the city of Évora, in the Lisbon region, in the Lower Tagus River Valley region, and along the Algarve coast (Ferrão et al. 2016). The greater Lisbon area is probably the zone with greater seismic risk, coincidently where the capital and largest city of Portugal is located. It is affected by the occurrence of large moment magnitude (M_w> 8) distant earthquakes and of medium magnitude (M_w> 6) near earthquakes (Azevedo et al. 2010). An example of a distant event is the 1755 earthquake (M_w > 8.5) generated in the Eurasian-Nubia plate boundary zone. However, local intraplate (M_w≈ 6–7) earthquakes have occurred more frequently, in 1344, 1531 and 1909.

The Portuguese National Annex of the European Standard for Design of structures for earthquake resistance, EN 1998-1, Eurocode 8 or EC8-NA (CEN 2010), established the seismic zonation of continental Portugal, as shown in Fig. 1. This zonation considers two types of seismic actions: Type 1 and Type 2. Type 1 refers to a "distant earthquake" scenario, corresponding to greater magnitude earthquakes at longer distances

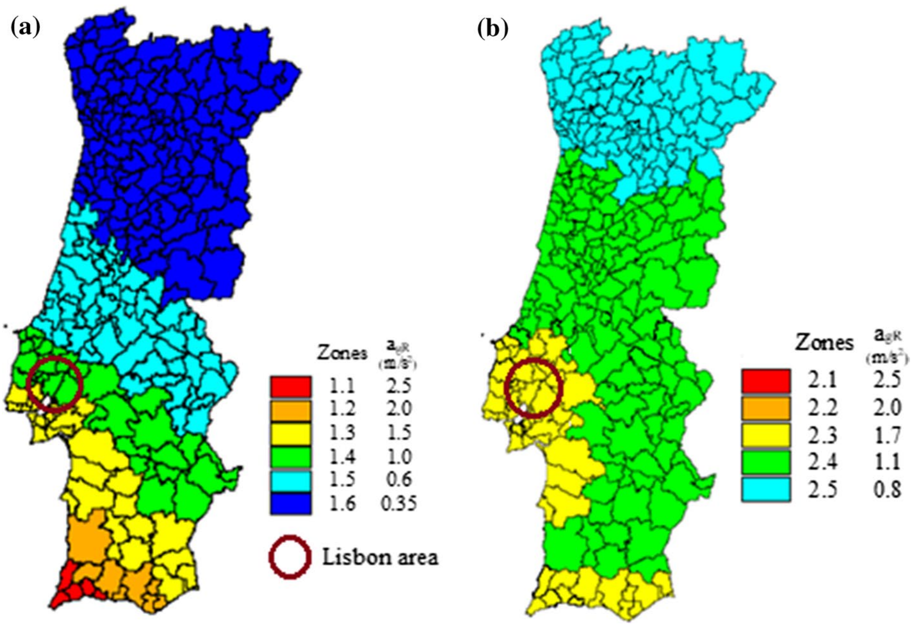

Fig. 1 Seismic zonation of Portugal mainland: **a** Action Type 1; **b** Action Type 2 (adapted from EC8)

(with epicentre in the Atlantic region), while Type 2 refers to a “near earthquake” scenario, associated with moderate magnitude earthquakes at close distance (with epicentre in the continental territory). According to EC8, seismic hazard is described in terms of the peak ground acceleration in type A ground (rock), a_{gR}. The values of a_{gR} for each zone and seismic action type are included in Fig. 1. Following these seismic actions, examples of liquefaction assessment by in situ tests are available in the Algarve (e.g. Rodrigues et al. 2016).

Earthquake Induced Liquefaction Disasters (EILDs) are responsible for significant additional structural damage and casualties, particularly in zones where specific geologic, geomorphological, hydrological and geotechnical characteristics indicate liquefaction potential of soils below structures (LIQUEFACT 2017). The presence of thick profiles of recent alluvial sandy deposits in a high seismicity area is a good example of the combination of the necessary liquefaction triggering conditions.

Information regarding seismic activity in Portugal only started being collected after the 1755 earthquake. For older events, the available data only include the testimonials of people experiencing large earthquakes. Since these are mostly subjective descriptions of ordinary people, it has been hard to assess the level of reliability of this information with reference to liquefaction; this means that doubts arise in several circumstances as to whether the phenomenon actually occurred. For this reason, as discussed by Jorge (1993), data in the catalogue are classified in terms of quality of information and localization of the source. In particular, the categories are ‘certain’, ‘doubtful’, ‘very doubtful’ and ‘credible’ liquefaction. The first three categories refer to descriptions directly related to liquefaction, with more or less certainty. The ‘credible liquefaction’ category provides information, not directly describing but potentially related to the liquefaction phenomenon. Following this approach, Jorge and Vieira (1997) identified in the map shown in Fig. 2, the locations of historical liquefaction events coupled with a reliability classification. This is considered the most reliable source of information on the evidences of the liquefaction phenomenon in Portugal. From the earthquake catalogue, Jorge and Vieira (1997) identified six earthquake events associated with liquefaction, as indicated in Fig. 2: 26/01/1531 ($M=7.1$); 01/11/1755 ($M=8.5$); 31/03/1761 ($M=7.5$); 12/01/1856 ($M=6.0$); 11/11/1858 ($M=7.2$) and 23/04/1909 ($M=6.6$). The details of these events are listed in Portuguese catalogues, including the magnitude, macroseismic intensity and coordinates of the epicentre. The locations where liquefaction occurred as well as the epicentral distances were not reported, but were assumed, according to the site where liquefaction was observed, even considering the large degree of uncertainty. This uncertainty was reflected in the calculation of the estimated epicentral distances, however the error made in this computation was taken into account.

A liquefaction potential zonation map of Continental Portugal was developed by Jorge (1993) and further discussed by Jorge and Vieira (1997). This zonation map was derived from the superposition and generalization of two basic maps: the liquefaction ‘opportunity’ map and the liquefaction susceptibility map. For the greater Lisbon area, a more detailed representation was produced, which evidenced the high liquefaction potential of that region, as illustrated in Fig. 3.

After the identification of the ‘high to very high’ liquefaction susceptibility areas in Fig. 3, mostly along the Lower Tagus Valley, the collection and analysis of existing geotechnical data in that region was carried out, mainly covering the municipalities of Vila Franca de Xira, Benavente, Montijo and Barreiro.

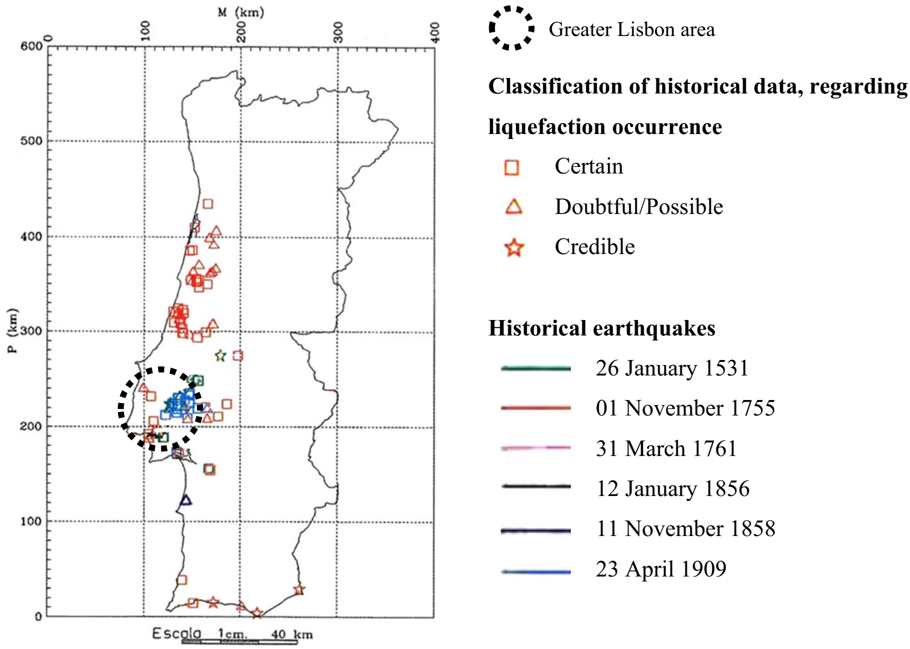

Fig. 2 Location of liquefaction events associated with historical earthquakes (adapted from Jorge 1993). Note: "Very doubtful" occurences have been removed from the original map. Permission granted by the author

2.2 Collection and analysis of existing information

For the selection of the location of the pilot site, the investigation was initiated with the collection of existing geological and geotechnical information in the metropolitan region of Lisbon along the Lower Tagus River Valley area. With the collaboration of numerous public institutions, governmental agencies, private companies, contractors and design offices, a considerable volume of geotechnical data was assembled. After careful inspection, 95 geotechnical reports were selected for analysis, in a total of more than 350 test results. The majority of these tests, about 72%, corresponded to SPT and borehole logging, in a total of 257 test results, but also included 70 CPT(u), 12 DMT and 17 V_S measurements (from SCPT, Cross-Hole or seismic refraction). Information on the position of the groundwater level at the time of testing was also available in most test reports.

These reports refer only to the North-East to South part of the Lower Tagus Valley in the Greater Lisbon, where quaternary sand deposits are expected, involving the municipalities of Vila Franca de Xira, Azambuja, Salvaterra de Magos, Benavente, Alcochete, Montijo and Barreiro, mostly located along the left bank of the Tagus river and estuary. Important works associated to the construction of a major highway (A10), including a 12 km extension bridge and viaduct crossing the river Tagus and agricultural plains, have provided a wealth of information from extensive geological and geotechnical site characterisation tests, which were collected and analysed for the present research.

For the assessment of liquefaction susceptibility in this region, the peak ground acceleration a_{max} was computed according to EC8-NA (CEN 2010), as summarised in Table 4.

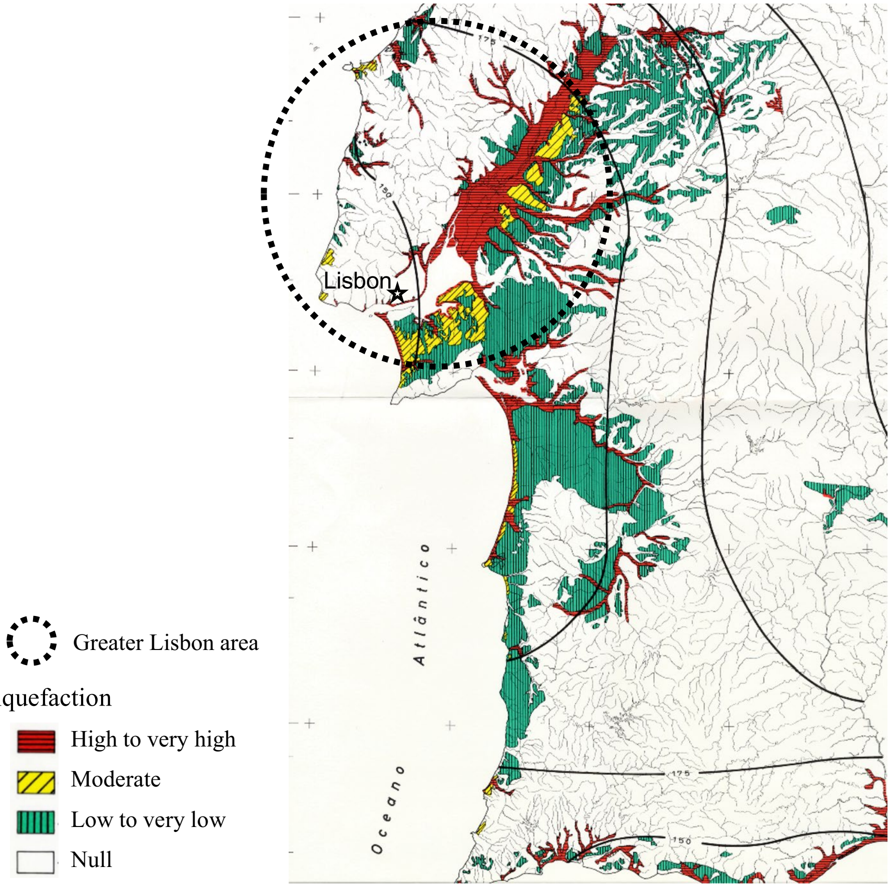

Fig. 3 Liquefaction zonation map (Jorge 1993; Jorge and Vieira 1997). Permission granted by the author

The analysis of the collected reports was carried out, according to the type of test, based on the previously described approaches to the assessment of liquefaction susceptibility. The classification of the liquefaction susceptibility of each soil profile was made, according to two criteria: (a) minimum factor of safety of 1.00; (b) minimum thickness of the liquefiable soil layer of 3 m. Consequently, three classes have been considered: low, moderate and high. For the purpose of geographical referencing and future microzonation, each test point was geographically located and colour-coded, according to the adopted colour scheme, introduced in Table 5. On a first approach, geo-referencing was made by introducing all coordinates on Google Earth®. In order to aid visual identification of liquefiable areas, the same colour code was associated with paddle icons for SPT data, diamond paddle icons for CPT data and target circles for CH (cross-hole) data, as schematically shown in Table 5.

This colour classification of SPT, CPT and CH data points has been superimposed on the liquefaction zonation map in Fig. 3 (from Jorge 1993), as illustrated in Fig. 4.

Despite some variability regarding liquefaction susceptibility, there is a substantial agreement between the general zonation map and the analysed data points. In effect, the red points in Fig. 4 are predominantly located in the area previously identified as having

Table 4 Calculation of a_{max} for Vila Franca de Xira and Benavente, according to EC8-NA (CEN 2010)

Seismic action	Seismic zone	M_w	a_{gR} (m/s^2)	γ_I	a_g (m/s^2)	Ground type	S_{max}	S	a_{max} (m/s^2)	a_{max} (g)
Type 1	'1.4'	7.5	1.0	1	1.0	D	2.0	2.00	2.0	0.20
Type 2	'2.3'	5.2	1.7	1	1.7	D	2.0	1.77	3.0	0.31

Table 5 Susceptibility colour code used for existing data points, based on the factor of safety to liquefaction (FS_{liq})

Susceptibility	Thickness of liquefiable soil layer	Colour code	SPT data	CPT data	CH data
None to Negligible	$FS_{liq} > 1$ ($h_{liq} = 0$ m)	Green			
Moderate	$FS_{liq} \leq 1$: $0 < h_{liq} < 3$ m	Orange			
High	$FS_{liq} \leq 1$: $h_{liq} \geq 3$ m	Red			

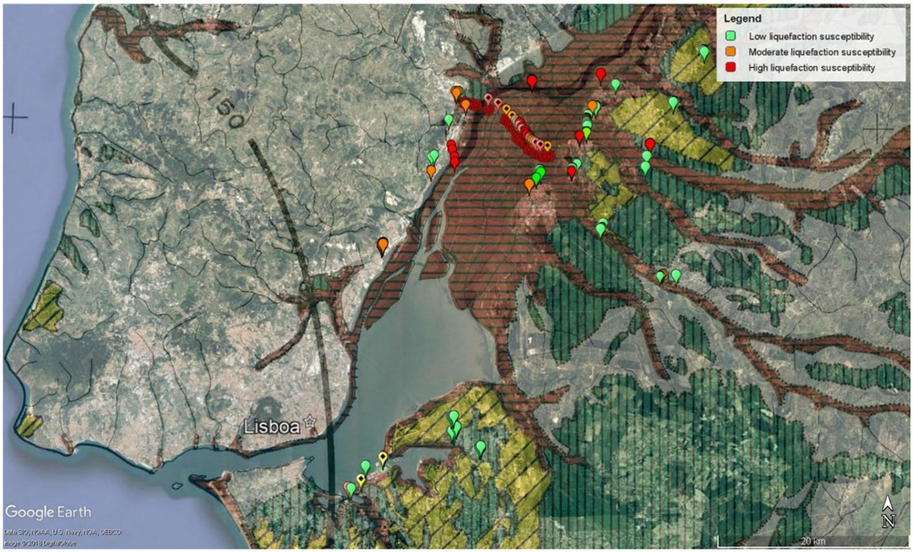

Fig. 4 Location of the geotechnical reports collected in the greater Lisbon area, superimposed on the existing liquefaction zonation map (from Jorge 1993)

high to very high liquefaction susceptibility, mainly involving the municipalities of Vila Franca de Xira and Benavente.

2.3 Location of the pilot site

The area in the agricultural plains of the "Lezíria Grande de Vila Franca de Xira" was found to have the ideal geological, hydrogeological and geotechnical, as well as operational conditions, for constituting a research pilot site on liquefiable soils. The area of the pilot site was divided into zones, named Site Investigation (SI) points, identified by the respective number. Table 6 summarises the number, type and location of the tests performed at the pilot site and in each SI, and Fig. 5 indicates the testing locations in a map. The location of each type of tests was selected based on a geological and geomorphological interpretation of the site, described in detail in Viana da Fonseca et al. (2017) and Saldanha et al. (2018). The position of the groundwater level was measured in each testing location, which is particularly relevant for liquefaction analyses. An extensive series of microtremor measurements was also performed, complementary to these investigations, for the purpose of the liquefaction microzonation of the region, which will not be addressed in this paper.

Table 6 Tests performed in the pilot site

Type of test	Number of tests	Location
Geotechnical		
SPT	2	SI1; SI7
CPTu	10	SI1, SI2, SI3, SI4, SI5, SI6, SI7, SI10, SI12, SI13
SDMT	3	SI7, SI8, SI9
Geophysical		
SASW	1	SI5
Cross-hole (CH)	2	SI1; SI7 (not considered, see text below)
Seismic refraction (SR)	8	SI1, SI5, SI6, SI7, SI9, SI11, SI12, SI13

Fig. 5 Location of the site investigation (SI) points and of the main tests at the pilot site

For the purpose of liquefaction susceptibility assessment from penetration tests, the analysis will focus on SPT, CPTu and DMT data. For Vs-based liquefaction analysis, direct measurements of SDMT and estimated values based on SPT, CPT and DMT results will be considered, since CH results were found to be unreliable due to equipment malfunctioning. On the other hand, surface geophysics results were applied for complementing the geological and geotechnical characterisation of the site, namely for layer detection, by effectively covering large areas. The predictions of shear wave velocities from the geotechnical tests were included, given its valuable contribution to liquefaction analyses, as detailed in Ferreira et al. (2018).

3 Characterisation of the pilot site

3.1 SPT results and preliminary liquefaction assessment

Two SPT tests were carried out in SI1 and SI7, respectively. High quality samples were collected in an adjacent borehole, using the Mazier sampler, for complementary laboratory studies. The SPT test results in the two locations in terms of $(N_1)_{60,cs}$ are presented in Fig. 6, together with a simplified soil profile defined from the SPT results, as well as a preliminary analysis for liquefaction susceptibility using the simplified procedure, considering Type 1 and 2 seismic actions. The resulting factors of safety against liquefaction refer only to the sandy layers.

For clearer perception of the evolution of the factor of safety, FS_{liq}, with depth, 3 coloured zones have been added, corresponding to values below 1.00 (red), between 1.00 and 1.25 (yellow) and above 1.25 (green). The value of 1.00 is conventionally, as previously stated, the minimum factor of safety; however, EC8 is more conservative, proposing a minimum FS_{liq} value of 1.25, hence the transition area in yellow.

In the illustrated cases of SI1 and SI7 in Fig. 6, it is clear that thick sandy layers exhibit high to very high liquefaction susceptibility, except for a medium dense sand layer at 5–8 m in SI1. Based on these SPT results, a preliminary liquefaction analysis of each location can be made. At SI1, a non-liquefiable clayey crust of about 2 m is followed by a 20 m thick liquefiable sandy layer, interbedded by a medium-dense sand layer between 5 and 8 m, after which a silty clay non-liquefiable layer was found. On the other hand, at SI7, the non-liquefiable clayey crust is 6 m thick and the liquefiable sandy layer is about 11 m thick, located between 6 and 17 m, followed by a clay layer. This analysis will be further discussed by comparison with other geotechnical data.

3.2 CPTu testing

In this pilot site, ten piezocone tests (CPTu) were performed. The tests were performed according to the ISO 22476-1.2012 (ISO 2012) and the normative procedures proposed by the TC16. The results were treated using the methodology of Boulanger and Idriss (2014) for soil liquefaction analysis, as previously introduced. The groundwater level was measured in each in situ test location, varying from 0.3 to 2.0 m. The in situ measured values were used in the calculations. Figure 7 shows an example of the CPTu results in three plots: (a) cone resistance (q_c) and pore pressure (u_2); (b) soil behaviour type index (I_c) and simplified soil profile; (c) liquefaction factor of safety (FS_{liq}).

The first plot (Fig. 7a) provides the basic information of the soil profile, allowing to distinguish the depths at which the soil layer is granular (higher cone resistance and pore pressure coincident with the hydrostatic line) or fine-grained (lower cone resistance and excess pore pressure). The I_c plot (Fig. 7b) illustrates a preliminary soil profile, based on the proposal of Robertson and Wride (1997); in addition, a simplified soil profile has been defined, by approximating the original I_c by constant values, where similar behaviour is expected. As proposed by Cubrinovski et al. (2017), the simplified soil profile considers: gravel and coarse sand ($I_c \leq 1.3$); clean sand ($1.3 \leq I_c \leq 1.8$); sands with low fines content ($1.8 \leq I_c \leq 2.1$); silty sand, sandy silt and non-plastic silt ($2.1 \leq I_c \leq 2.6$); and, non-liquefiable silt or clay ($I_c \geq 2.6$). This soil classification is different from the original classification proposal from Robertson (1990), updated by Robertson (2009), as it is focused on

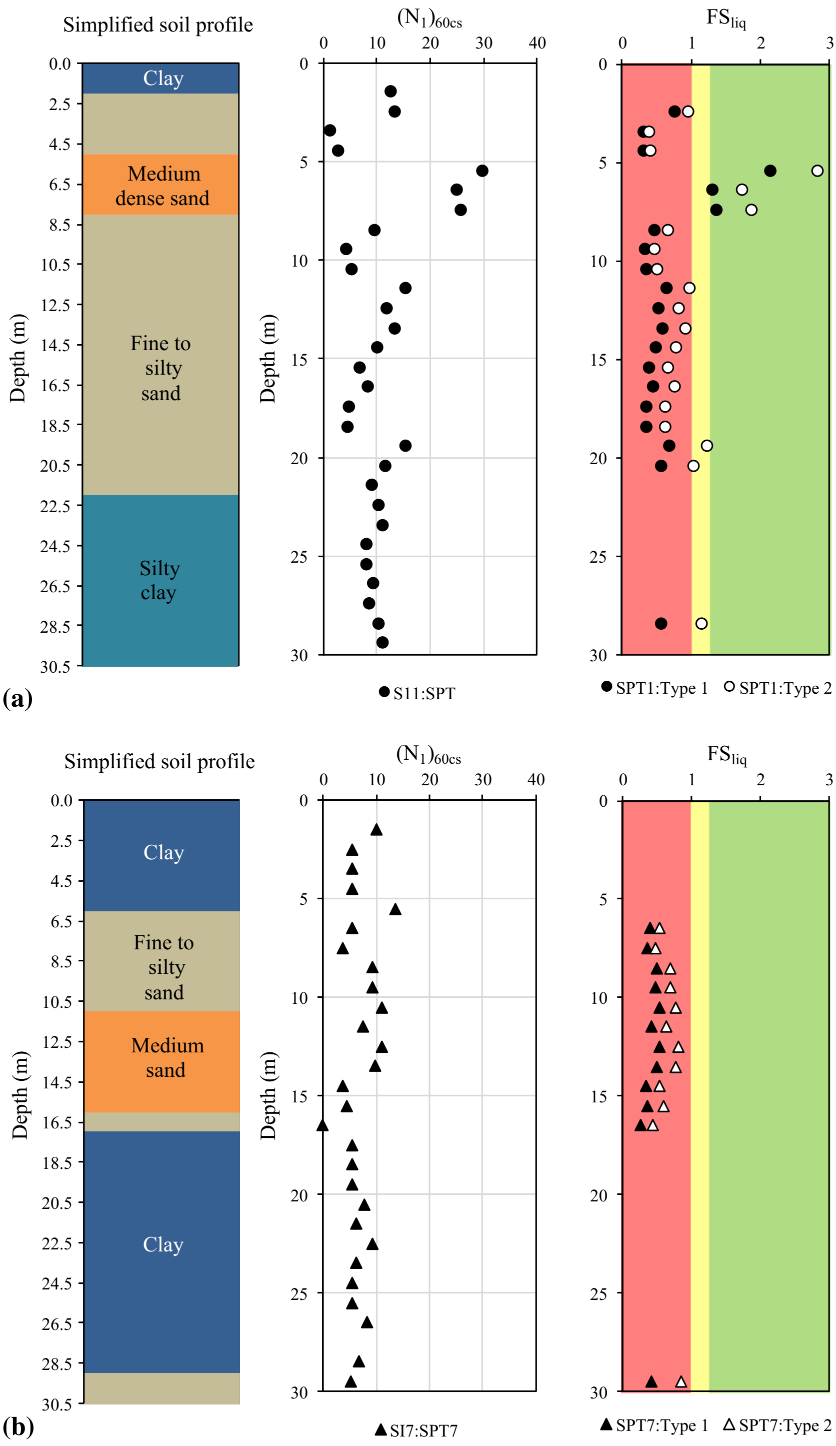

Fig. 6 SPT-based assessment of liquefaction potential at the pilot site: **a** SI1, **b** SI7

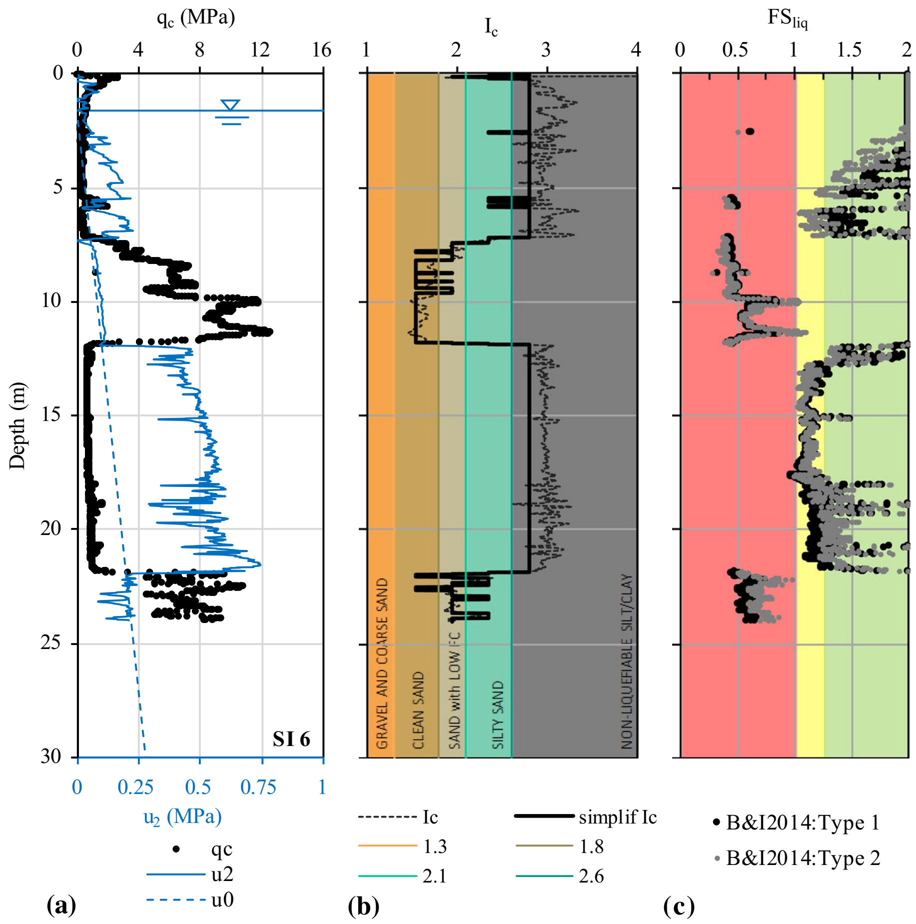

Fig. 7 CPTu results in the pilot site at SI6

soil response with respect to earthquake-induced liquefaction. From this point of view, there is no distinction between silts, clays and organic or sensitive soils; instead, these soil types have been grouped together as non-liquefiable soils. On the other hand, sands have been sub-divided to account for different fines content: from clean sand to low FC sands, to silty sands, since liquefaction case histories suggest that small variations in fines content strongly influence liquefaction susceptibility. Finally, Fig. 7c illustrates the variation of the factor of safety against liquefaction, FS_{liq}, in depth. Again, coloured zones have been included to ease identification of the critical layers: red for values below 1.00, yellow between 1.00 and 1.25 and green for values above 1.25.

In the case of SI6, shown in Fig. 7, the simplified I_c plot shows distinct soil layers, which can be clearly identified and summarised as follows: a top non-liquefiable layer about 7 m thick, followed by a 5 m thick clean sand layer down to 12 m, then a non-liquefiable layer down to 22 m and a deeper soil layer, consisting of sands with low fines content, again with high liquefaction susceptibility. It should be noted that, below 20 m, liquefaction evaluation is less reliable and should be analysed by means of specific site response analyses, since the uncertainty in some of the computation factors becomes larger (Boulanger and Idriss 2014).

A general overview of 6 CPTu at different locations within the pilot site are plotted in Fig. 8. Thick liquefiable layers can be identified in all of these profiles, despite the significant variability in depth among the different testing locations.

3.3 SDMT testing

In this pilot site, four Seismic Flat Dilatometer tests (SDMT) were performed in the first stage, according to Eurocode 7-Part 3 recommendations and ISO/TS 22476-11. However, at SI1, operational problems were experienced, having reached a depth of only 4 m. The seismic dilatometer is an extension of the traditional DMT, introduced by Marchetti (1980) with a seismic module implemented above the steel blade (Marchetti et al. 2008). The seismic module consists of an instrumented rod connected between the DMT blade and the rods, equipped with two horizontal geophones spaced 0.50 m, for measuring shear wave velocities, V_S. The presented DMT results were obtained directly from the usual DMT interpretation formulae according to Marchetti (1980) and Marchetti et al. (2001). In this respect, Fig. 9 shows the profiles of the material index I_D (indicating soil type) and of the horizontal stress index K_D (related to the stress history) together to the corresponding liquefaction safety factor FS_{liq} at the investigation sites, namely SI7, SI8 and SI9. At each of the sites, FS_{liq} was calculated using the Marchetti (2016) CRR-K_D correlation (DMT data only), while at SI7 DMT and CPT results were combined, according to the Marchetti CRR-K_D-Q_{cn} formulation.

Comparing with CPT results, DMT liquefaction assessment also detects a non-liquefiable silty-clayey crust of 3 to 6 m thickness, depending on the site investigation location, before encountering the sandy and silty-sandy deposits that provide most of the liquefaction down to 14–16 m depth. The combined use of CPT and DMT in SI7 follows the same DMT tendency, even though the liquefaction susceptibility appears to be much lower, probably due to the presence of interbedded layers that do not allow a correct coupling of DMT and CPT data at certain depths.

3.4 Geophysical investigations

Seismic wave velocities were measured in the pilot site by means of geophysical surface wave methods, namely via seismic refraction (SR), spectral analysis of surface waves (SASW), as well as in borehole tests, such as the seismic dilatometer (SDMT) and cross-hole (CH) tests. For the purpose of liquefaction assessment, the results of seismic refraction tests were also considered, despite being better suited for profiling and layer detection, by identifying changes in seismic wave velocities in depth. However, borehole seismic tests are considered more reliable and detailed and were analysed, based on direct measurements of V_S, as well as its prediction from penetration tests. In effect, from the variety of in situ penetration tests performed at the pilot site, it was possible to obtain predictions of V_S from correlations with SPT, CPTu and DMT test results. For the SPT-Vs correlations, the proposals of Wair et al. (2012) for different soil types were used, which also take into account the effective vertical stress at each depth of the soil profile. For CPT-V_S correlations, the proposals of Hegazy and Mayne (1995), Mayne (2006), Andrus et al. (2007), Robertson (2009) and Monaco et al. (2005) were analysed. As detailed in Ferreira et al. (2018), the prediction proposed by Robertson (2009) was

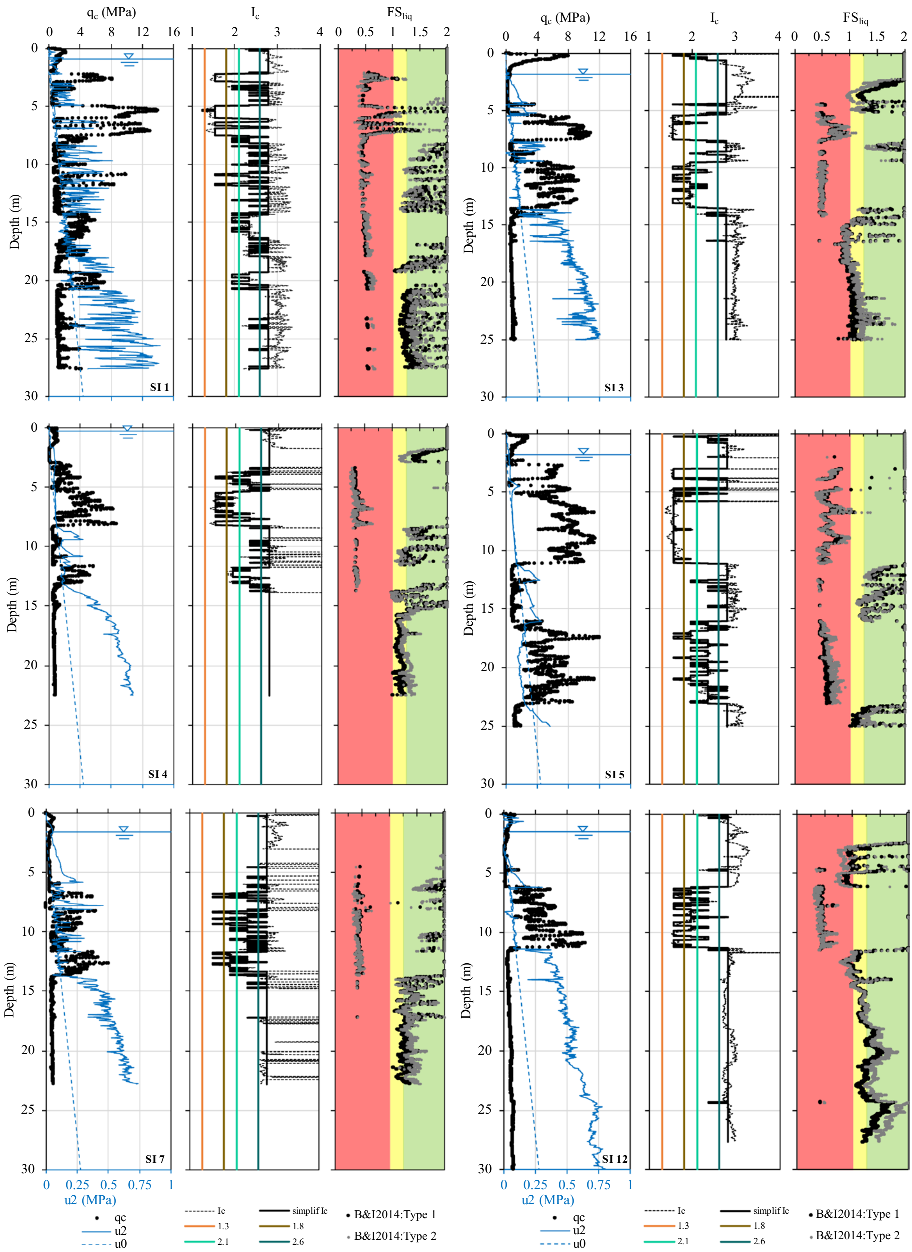

Fig. 8 Selection of CPTu results in the pilot site at SI1, SI3, SI4, SI5, SI7 and SI12

found to be the most appropriate for these soils. For V_S predictions based on DMT, the proposal of Marchetti et al. (2008) was adopted. Amoroso (2014) demonstrated that the DMT-based predictions are more consistent than those based on the CPT. For this

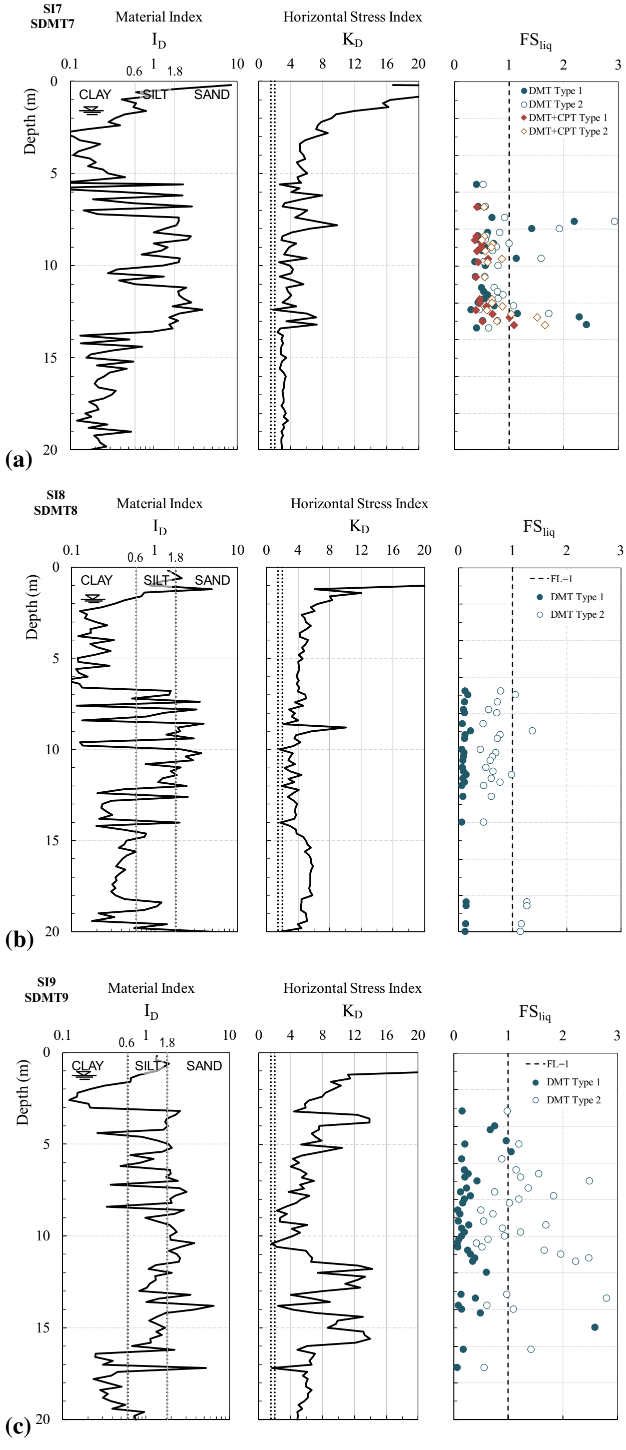

Fig. 9 SDMT results in the pilot site: **a** SI7, **b** SI8, **c** SI9

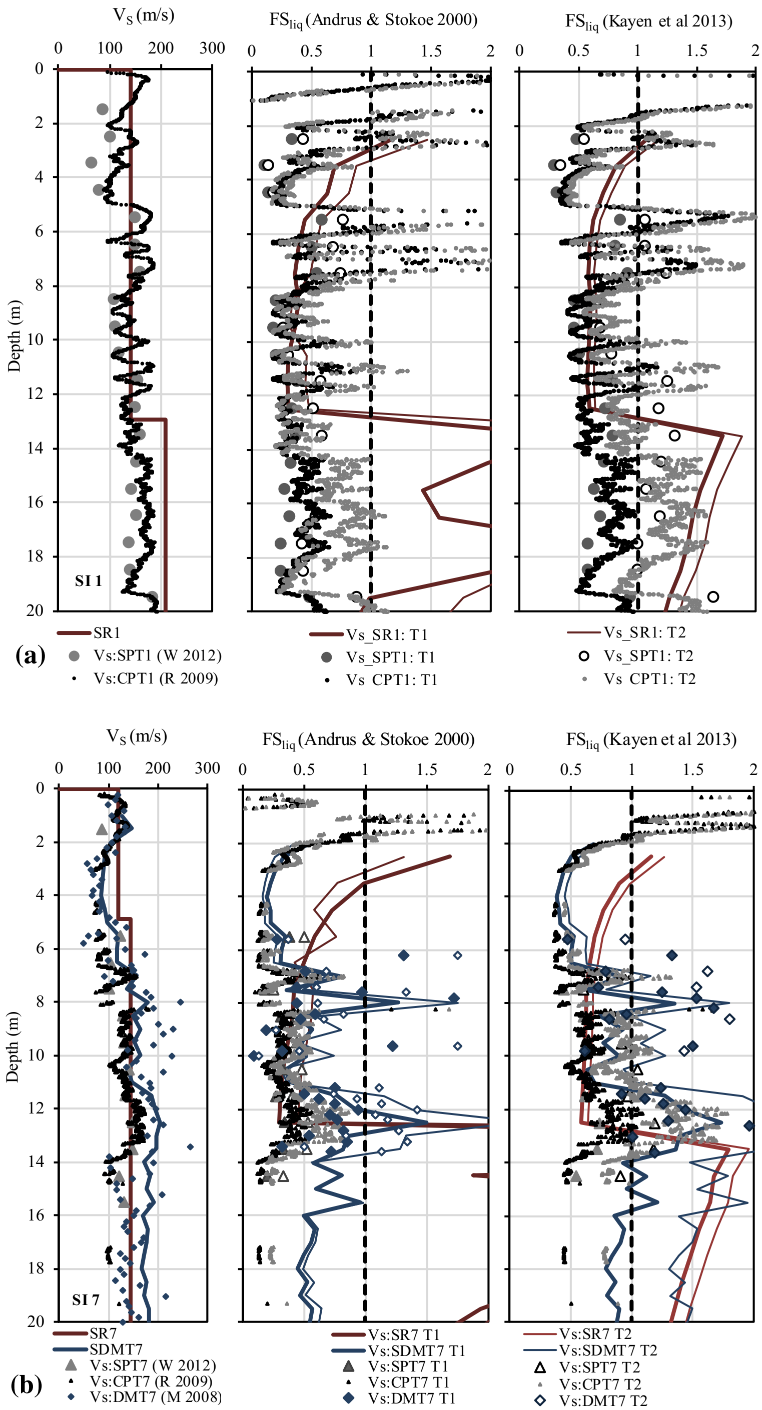

Fig. 10 Measured and estimated V_S results and respective FS_{liq}: **a** SI1, **b** SI7

analysis, Fig. 10 presents the results obtained at SI1 and SI7, in terms of measured V_S via SR and SDMT, as well as estimated V_S profiles based on:

- Wair et al. (2012): SPT (W 2012)
- Robertson (2009): CPT (R 2009)
- Marchetti et al. (2008): DMT (M 2008)

Figure 10 also includes the computed factors of safety against liquefaction using the two distinct approaches: Andrus and Stokoe (2000) and Kayen et al. (2013) for the two seismic actions (T1 and T2), taking into account the estimated fines content.

In both locations, the results show significant approximation between measured and predicted V_S values. As expected, seismic refraction provides simplified profiles, assuming a stiffness increase with depth, which is not always the case in SI7, as shown in the SDMT profile. DMT-based predictions are remarkably similar with SDMT measurements, which demonstrates the good performance of Marchetti et al. (2008) proposal. As evidenced by Amoroso (2014), DMT-based predictions appear to be more consistent than those based on the CPT considering that DMT-V_S correlations include the horizontal stress index K_D, noticeably reactive to stress history, prestraining/aging and structure, scarcely detected by cone tip resistance q_c from CPT. On the other hand, CPT-V_S predictions are subjected to the additional uncertainty arising from the selection of which one of the numerous existing correlations is adopted, depending on geological age, cementation, effective stress state. With regard to the liquefaction susceptibility assessment, the obtained FS_{liq} values are indicative of very thick liquefiable soils at both locations. However, in SI7, there are significant discrepancies in the results, which are likely linked to the soil type consideration and estimate of fines content, based on FC, I_C and I_D, respectively.

4 Analysis and discussion

4.1 Combining field and laboratory data

For comparing the results of these field tests, especially in terms of liquefaction susceptibility assessment, two site investigation locations were selected: SI1 and SI7. In order to specifically address the impact of soil type, especially fines content, the laboratory results of grain size distribution and plasticity, obtained on SPT samples, have been integrated in the SPT-based liquefaction assessment. Figure 11a shows the first 20 m of the simplified soil profile in SI1, and Fig. 11b presents the comparison between the SPT-estimated and laboratory measured fines content and plasticity index. The SPT-estimated FC were defined, considering the proposal by Idriss and Boulanger (2004, 2010), and based on the lithological description of the SPT log (below 5% for clean sand; 5–10% for sand with fines; 10–30% for silty sand; above 30% for fine non-liquefiable soils). In addition, the soil type parameter I_C from CPTu, with a cut-off at 2.35 (average value between 2.1 and 2.6) corresponding to the midpoint between silty sands and non-liquefiable soils, is provided in Fig. 11c. The combination of field and laboratory data enabled to redefine the soil profile, by identifying the sandy layers, potentially susceptible to liquefaction, as illustrated in Fig. 11d.

The most striking observation, at first glance, is that the revised soil profile is more complex and stratified than the simplified profile derived from the lithological description

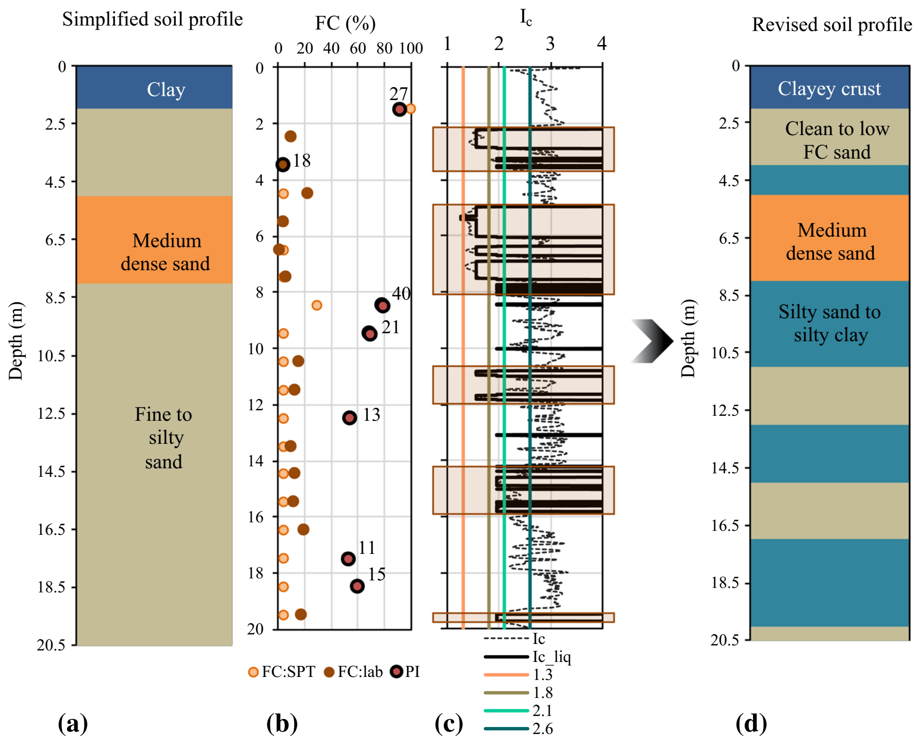

Fig. 11 SI1 results: **a** SPT simplified soil profile based on lithology; **b** SPT-estimated and lab-measured fines content; **c** simplified I_C for liquefaction; **d** revised soil profile. Note: where PI is not specified means non-plastic (NP) soil

of the SPT. This is due to the laboratory measurement of fines content, which provides a very different outline of the soil type, as shown in Fig. 11b. In this figure, the plasticity indexes at different depths are also included, which are relevant in liquefaction analyses (Boulanger and Idriss 2014). It is clear that the SPT test alone fails to identify the existence of clay/silt layers interbedded with the sand deposits, which have a very significant impact in the liquefaction response of the profile, so the use of complementary information, especially from the laboratory analysis of the collected SPT samples, is highly beneficial.

Based on this revised soil profile and using the laboratory-measured fines content information, the factors of safety against liquefaction obtained from SPT, as well as from the estimated V_S-SPT and V_S-CPT profiles (Kayen et al. 2013 approach) have been recalculated, as indicated in Fig. 12, from which the critical layers can be easily identified. In addition, the CPTu profile has also been revised, by removing FS_{liq} values for I_C above 2.35 (midpoint between silty sands and non-liquefiable soils). For clarity, the results from seismic refraction tests were not included in this comparison.

In contrast with the FS_{liq} profiles in Figs. 6a and 8 (SI1), the consideration of the adjustments in fines content enabled a clearer distinction between layers, particularly useful in the identification of the critical ones. In this case, a layer of moderate to low liquefaction susceptibility was also detected. Despite the larger scatter in the V_S-based FS_{liq} profiles, the same critical layers can be recognised, mainly for T1 seismic action. For the lower

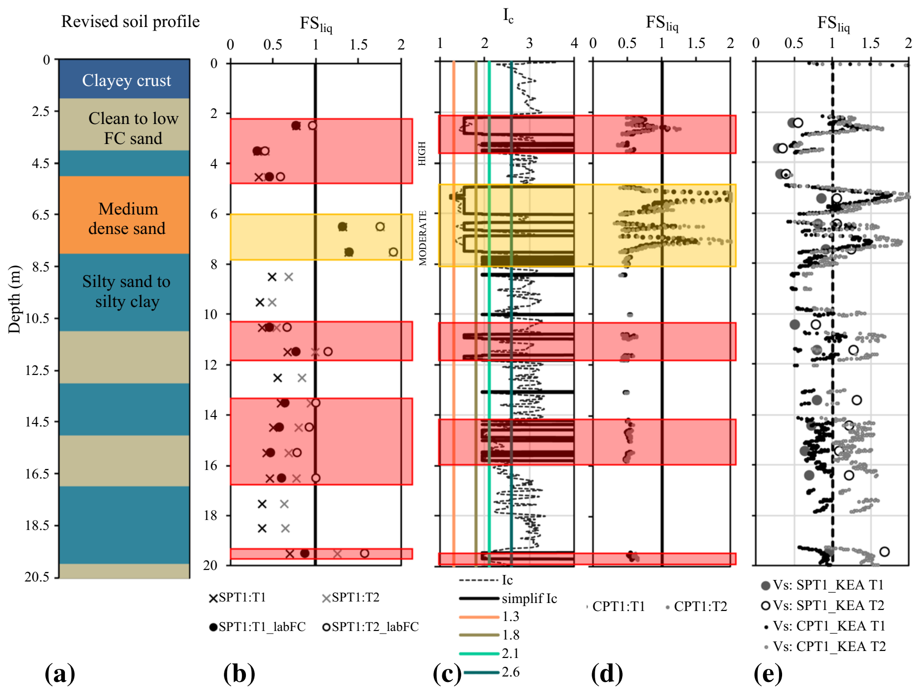

Fig. 12 Identification of critical layers in SI1 taking FC into account: **a** revised soil profile, **b** SPT FS_{liq}, **c** revised Ic, **d** CPTu FS_{liq}, **e** V_S FS_{liq}

magnitude seismic demand (T2), the V_S-FS_{liq} profiles are substantially higher, suggesting that the computed DWF (Distance Weighting Factor, similar to MSF) may need further adjustments.

In sum, in this location, three highly liquefiable layers have been identified, between 2 and 5 m, then at 10–12 m, and then from 13 to 17 m. A very thin deep liquefiable layer was also found nearly at 20 m, which effect at the surface is expected to be negligible. Since the SPT and CPT tests were performed very close to each other, the discrepancies in the results can only be attributed to the nature and specificities of the in situ test, as it is necessarily the same soil profile. Since the CPT measurements are nearly continuous (every 1 cm), while the SPT was performed at every 1 m in depth, the observed differences are a reflection of the many intercalations of fine layers, which often are not visible in the SPT results. In fact, the CPT results show some points where the FS is high, as well as the SPT results. What is apparent from this comparative analysis is that the greater detail of the CPT is fundamental to identify these heterogeneous soil profiles, while the SPT may lead to a different perception of the soil profile.

For the second site at SI7, a similar analysis was performed, as outlined in Fig. 13, with simplified SPT soil profile of the first 20 m (Fig. 13a), the SPT-estimated (from the lithological description of the SPT log) and lab-measured fines content (Fig. 13b), CPTu soil type profile from I_C ((Fig. 13c). Combining this information, a revised soil profile has been produced (Fig. 13d).

In this case, the original soil profile has been converted into a simpler three-layered profile, despite the existence of thin interbedded layers of finer soil, as noted in the soil

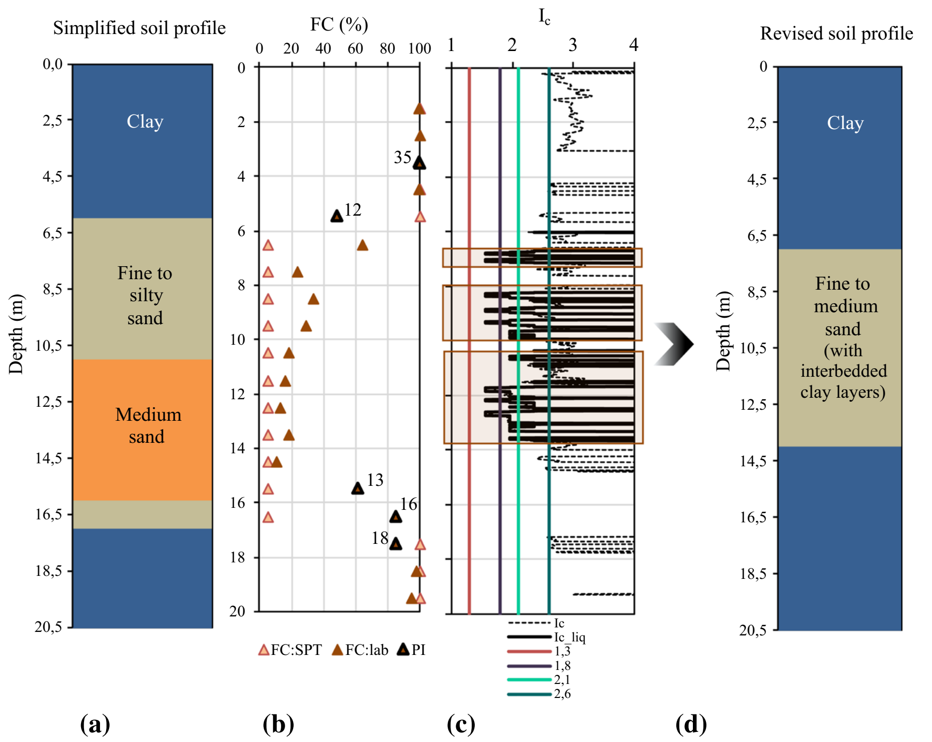

Fig. 13 SI7 results: **a** SPT simplified soil profile based on lithology, **b** SPT-estimated and lab-measured fines content, **c** simplified I_C for liquefaction, **d** revised soil profile. Note: where PI is not specified means non-plastic (NP) soil (for FC < 50%)

type description. The comparison between SPT-estimated and laboratory-measured fines content reveals clear differences, as before, particularly near the interface of the layers. The integration of this information in the revised computation of the factors of safety is illustrated in Fig. 14, which also includes the identification of the critical layers in terms of liquefaction susceptibility.

In this location, the simplified soil profiles from SPT and CPT are relatively similar, with two clayey layers at the crust and below about 16 m, and a central critical zone. However, the estimate of the thickness of the sandy layers slightly differs: the SPT results identified about 10 m of liquefiable sands (between 5 and 15 m), while the CPT indicates about 7 m of sandy soils (from 7 to 14 m), with a few interbedded layers of fine soil. In turn, DMT results suggest that the liquefiable layer is about 9 m thick, located from 5 to 14 m in depth. As highlighted in the figure, the combination of these results suggests that it is reasonable to consider a thick liquefiable layer, approximately between 6 and 15 m. With regard to V_S-based FS_{liq} results, a good agreement with the previous plot is evident, especially after the FC adjustment obtained from the laboratory measurements (by comparison with the V_S-FS_{liq} profile in Fig. 10b). It is again discernible that the inclusion of soil type information, such as from laboratory analyses, is vital to obtain a reliable V_S-based assessment of liquefaction susceptibility, clearly improving its capability for identifying liquefiable and non-liquefiable soil layers.

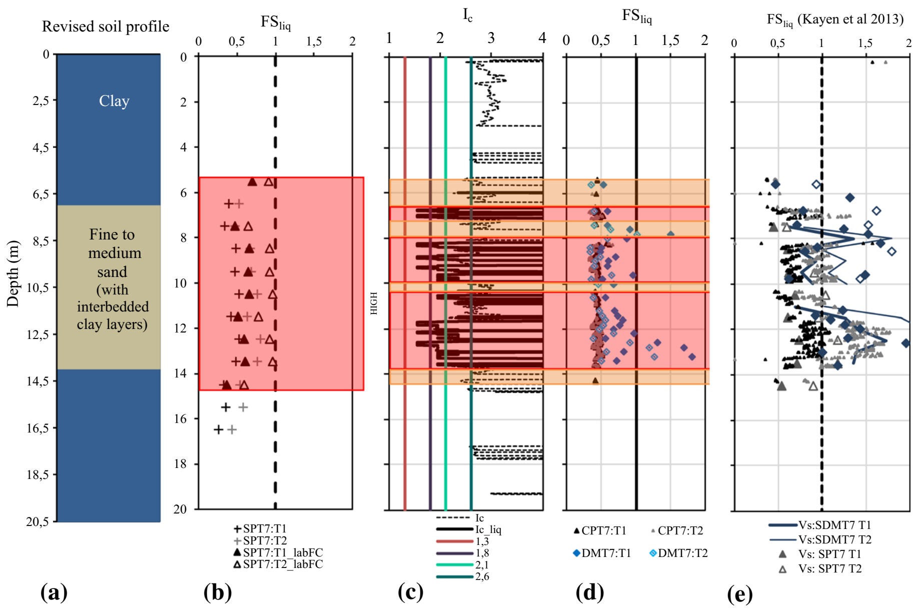

Fig. 14 Identification of critical layers in SI7 taking FC into account: **a** revised soil profile, **b** SPT FS_{liq}, **c** revised Ic, **d** CPTu and DMT FS_{liq}, **e** V_S FS_{liq}

4.2 Overview of the liquefaction response of the pilot site

As discussed in the introduction, the use of alternative and quantitative liquefaction indexes is advocated, providing relevant information in terms of the damage induced by soil liquefaction. For this purpose, LPI and LSN values have been computed, from the field penetration test data, namely SPT, CPT and DMT. At first, it is worth comparing all the results obtained at the pilot site from CPT data, as presented in Fig. 15. In this figure, LPI and LSN have been calculated considering the two types of seismic actions and a coloured background shading has been included, based on the classification of Tables 1 and 2.

As shown in Fig. 15, LPI values fall on the high or very high liquefaction severity, except for SI2 and SI13, where the LPI is low. SI4 appears to be the location with the highest liquefaction susceptibility, in terms of LPI, but SI5 and SI12 are also classified as highly liquefiable. In sum, from LPI results, it can be concluded that the majority of testing points exhibit high (50%) to very high (30%) liquefaction severity. In turn, based on the LSN results in Fig. 15, greater surficial liquefaction-induced damages are expected in SI4 and SI5, however the values fall within the moderate to severe class, that is, below 40. In terms of the variability of LSN values, there is greater scatter in its classification, with about 20% of the testing points in each class. Since LPI and LSN are liquefaction severity indicators, some authors have proposed a parallelism between them, namely Wotherspoon et al. (2015), who made use of the observed superficial manifestations after the Christchurch series of earthquakes to establish the comparison. The proposed classification relationship is provided in Table 7.

However, the results in Fig. 15 do not fit well within the relationship between LPI and LSN proposed in Table 7, mainly because the LSN values are relatively low, classifying liquefaction severity at all testing locations as minor to moderate, in relation to the relative

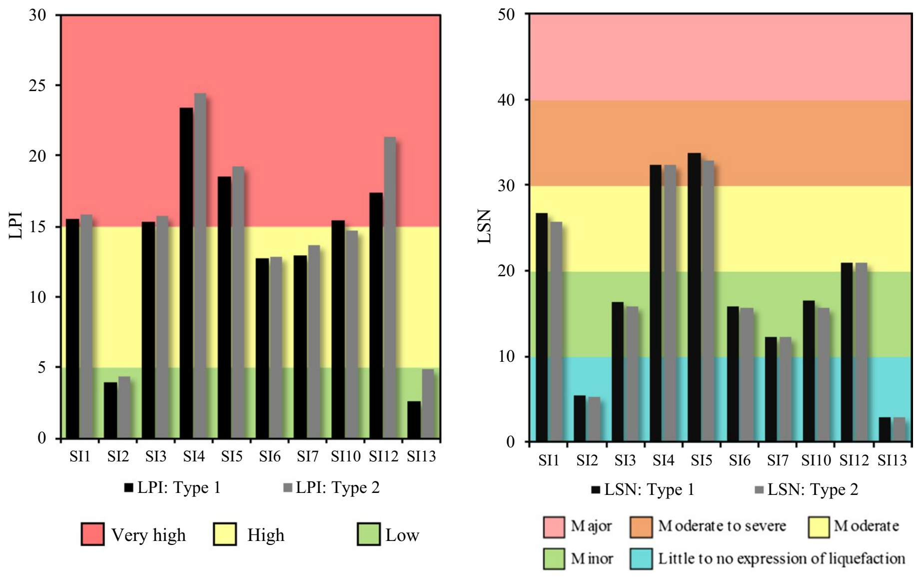

Fig. 15 Severity damage based on LPI and LSN from CPTu at the pilot sites

Table 7 Classification of liquefaction severity and damage based on LPI and LSN

Risk index	Superficial manifestation severity		
	None to minor	Moderate	Major to severe
LPI	LPI < 5	5 < LPI < 15	LPI > 15
LSN (Wotherspoon et al. 2015)	LSN < 20	20 < LSN < 50	LSN > 50
LSN (based on these results)	LSN < 10	10 < LSN < 20	LSN > 20

LPI, which indicates most testing locations as severely affected by liquefaction. Based on the available information, it is not yet possible to state which severity index is being poorly estimated at the pilot site, though it appears that LPI is over-conservative and LSN is possibly unconservative. This poor correspondence, also observed by Wotherspoon et al. (2015) and Cubrinovski et al. (2017), suggests that further studies are required, not only in terms of the liquefaction assessment procedures from which these indices are computed, but also to account for the configuration of the soil profile, namely the thickness of the crust, the depth and thickness of the liquefiable layers, as well as the relative distribution of liquefiable layers and interbedding with fine non-liquefiable layers (Millen et al. 2019). An adjustment based on these test results to the LPI versus LSN classification is also included in Table 7.

It is also interesting to compare these CPT-derived indexes with those from SPT, DMT, DMT combined with CPT tests, as well as from direct V_S measurements, summarised in Table 8 for LPI and LSN. The results show considerable differences between the absolute values of LPI and LSN, according to the type of test from which these have been computed.

These results suggest that the use of SPT data and V_S measurements for LPI or LSN estimates may lead to significant deviation from realistic values, especially in the presence

Table 8 Comparison of LPI and LSN values from SPT, CPTU and SDMT at SI1 and SI7

Seismic action	Type of test	LPI		LSN	
		SI1	SI7	SI1	SI7
Type 1	SPT	27.8	22.7	53.7	23.1
	SPT_lab FC	20.3	15.2	45.9	12.0
	CPT	15.58	12.95	26.74	12.17
	DMT	–	9.65	–	12.30
	DMT + CPT	–	7.70	–	10.25
	V_S_AS*	–	43.12	–	–
	V_S_KAE	–	26.19	–	–
Type 2	SPT	28.7	24.9	54.0	23.1
	SPT_lab FC	21.4	16.3	46.3	12.0
	CPT	15.88	13.72	25.79	12.17
	DMT	–	5.47	–	10.90
	DMT + CPT	–	4.88	–	9.54
	V_S_AS	–	42.78	–	–
	V_S_KAE	–	18.09	–	–

*V_S_AS (Andrus and Stokoe 2000); V_S_KAE (Kayen et al. 2013)

of interbedded layers of sands and silty clays, as in the present case. Both the original and revised values of SPT-FS_{liq} have been included (SPT and SPT_lab FC, respectively) to demonstrate the positive impact of the use of laboratory analyses of SPT samples in the improvement of SPT-derived parameters. From a qualitative perspective, the values from SPT and CPTu indicate similar trends, with higher values at SI1. On the other hand, the values of LPI and LSN obtained from DMT and CPT predictions appear reasonably similar, while the combined use of DMT and CPT provides lower indexes, probably due to the abovementioned interbedded layers that does not allow the correct coupling of DMT and CPT data at each soil depth. Given the inadequacy of V_S to distinguish between sandy and clayey soils, the use of V_S-based liquefaction indexes should only be used when specific soil type information (grain size distribution and index properties from laboratory analyses or I_C from CPTu) are available, otherwise these can be largely overestimated. The combination of V_S results with other geotechnical data on soil type proved to be a reasonable alternative solution to overcome this limitation. However, the corresponding LPI values are still overestimated in comparison with those from CPTu.

5 Conclusions

A new pilot site in liquefiable soils has been setup in the Greater Lisbon area, which has provided a wealth of geological, geophysical and geotechnical data to be explored and analysed, mainly in terms of liquefaction assessment protocols. The selection of its location is discussed in detail, based on the collection and analysis of existing geological and geotechnical reports. The conventional approach to liquefaction susceptibility assessment, based on the simplified procedure applied to SPT, CPT, DMT and V_S measurements, has been implemented, in terms of the factors of safety against liquefaction (FS_{liq}). The investigated area is constituted by very heterogeneous soil profiles, with interbedded sand-silt–clay layers. In some locations, more homogeneous layers of sand were found and some critical layers were identified, at different depths. However, the profiles are generally very heterogeneous, which is why the use of different in situ tests is even more relevant. In both SI1 and SI7, thick potentially liquefiable layers were found, as well as in many others (see Fig. 8) so it can be concluded that the pilot site area is prone to liquefaction.

Due to the presence of interbedded layers of sand and clayey soils, some discrepancies were observed in the results, particularly from direct interpretation of SPT and V_S results. This is a consequence of the lack of specific information on soil type, namely fines content, from these test results, which has a strong impact in the assessment of liquefaction susceptibility. To overcome these limitations, laboratory data from physical identification and grain size distribution obtained on SPT samples, were combined with field data, which considerably improved the convergence and the consistency of different test results. In effect, after the inclusion of laboratory measured fines content, it was possible to clearly identify the critical, highly liquefiable layers from the different tests. The analysis was complemented with alternative quantitative measures of the superficial damage induced by liquefaction, such as the Liquefaction Potential Index (LPI) and the Liquefaction Severity Number (LSN).

The main conclusion of this paper is that the use of different methodologies for the assessment of liquefaction susceptibility by means of in situ tests is beneficial, particularly if complemented with simple laboratory analyses of grain size distribution and consistency limits. This approach enabled to overcome the limitations of some of the approaches, particularly from SPT and V_S measurements. For the case study of this paper, which involved sensitive loose granular soils, often interbedded with finer soil layers, the laboratory information proved to be of great value to eliminate some discrepancies obtained by the conventional method on SPT data and V_S measurements. However, some discrepancies have not been resolved, evidenced by the LPI and LSN values, since the results from SPT_labFC are still considerably different from CPT results. The presence of many interbedded sand-silt–clay layers was found to compromise an accurate SPT evaluation of the liquefaction potential of the profiles, since the discrete 1-m data points of the SPT are often not representative. In short, the combination of these criteria enabled to identify the areas potentially most affected by liquefaction. Subsequent investigation campaigns are being carried out to refine the database and the results are currently being transferred to geo-statistical modelling software for the microzonation of the pilot site. Complementary information can be found in Viana da Fonseca et al. (2018), Ferreira et al. (2018), Saldanha et al. (2018) and Millen et al. (2019).

Acknowledgements LIQUEFACT project ("Assessment and mitigation of liquefaction potential across Europe: a holistic approach to protect structures/infrastructures for improved resilience to earthquake-induced liquefaction disasters") has received funding from the European Union's Horizon 2020 research and innovation programme under grant agreement No. GAP-700748. Acknowledgements are also due to the Portuguese stakeholders of LIQUEFACT, namely Teixeira Duarte, LNEG, ENMC, CMMontijo, CMBenavente, ABLGVFX, BRISA, CENOR, GEOCONTROLE and COBA, as well as to Dr. Luca Minarelli and Dr. Rui Carrilho Gomes. The second and third authors have received funding from FCT (Portuguese Foundation for Science and Technology) in the form of the SFRH/BPD/120470/2016 and SFRH/BD/120035/2016 grants, respectively.

References

Amoroso S (2014) Prediction of the shear wave velocity Vs from CPT and DMT at research sites. Front Struct Civ Eng 8(1):83–92. https://doi.org/10.1007/s11709-013-0234-6

Andrus RD, II Stokoe KH (2000) Liquefaction resistance of soils from shear-wave velocity. J Geotech Geoenviron Eng 126(11):1015–1025

Andrus, RD, II Stokoe KH, Juang CH (2004) Guide for shear-wave-based liquefaction potential evaluation. Earthquake Spectra 20(2):285–308
Andrus RD, Mohanan NP, Piratheepan P, Ellis BS, Holzer TL (2007) Predicting shear-wave velocity from cone penetration resistance. In: Proceedings of 4th international conference on earthquake geotechnical engineering, Thessaloniki, Greece
Azevedo J, Guerreiro L, Bento R, Lopes M, Proença J (2010) Seismic vulnerability of lifelines in the greater Lisbon area. Bull Earthq Eng 8:157
Boulanger RW, Idriss IM (2014). CPT and SPT based liquefaction triggering procedures. Report No. UCD/CGM-14/01. Center for Geotechnical Modeling, University of California, Davis
CEN (2010) Eurocode 8: Design of structures for earthquake resistance
Cubrinovski M, Rhodes A, Ntritsos N, Van Ballegooy S (2017) System response of liquefiable deposits. In: Proceedings of the 3rd international conference on performance-based design in earthquake geotechnical engineering, Vancouver, 16–19 July 2017
Ferrão C, Bezzeghoud M, Caldeira B, Borges JF (2016) The seismicity of portugal and its adjacent atlantic region from 1300 to 2014: maximum observed intensity (MOI) map. Seismol Res Lett 87(3):743–750. https://doi.org/10.1785/0220150217
Ferreira C, Viana da Fonseca A, Saldanha AS, Ramos C, Amoroso S, Minarelli L (2018) Estimated versus measured Vs profiles and Vs30 at a pilot site in the lower Tagus Valley, Portugal. In: Proceedings of the 16th European conference on earthquake engineering, Thessanoliki, 18–21 June 2018, ID: 10591
GeoLogismiki (2017) https://geologismiki.gr/products/cliq/. Accessed in November 2017
HegazyYA, Mayne PW (1995) Statistical correlations between VS and cone penetration data for different soil types. In: Proceedings of the international symposium on cone penetration testing, CPT'95, pp 173–178
Idriss IM (1999) An update to the Seed-Idriss simplified procedure for evaluating liquefaction potential. In: Proceedings of the TRB workshop on new approaches to liquefaction, Federal Highway Administration
Idriss IM, Boulanger RW (2004) Semi-empirical procedures for evaluating liquefaction potential during earthquakes. In: Doolin D et al (eds) Proceedings, 11th international conference on soil dynamics and earthquake engineering, and 3rd international conference on earthquake geotechnical engineering, vol 1. Stallion Press, pp 32–56
Iwasaki T, Tokida K, Tatsuoka F, Watanabe S, Yasuda S, Sato H (1982) Microzonation for soil liquefaction potential using simplified methods. Proceedings of 3rd international conference on microzonation, vol 3. Seattle, pp 1319–1330
Idriss IM, Boulanger RW (2006) Semi-empirical procedures for evaluating liquefaction potential during earth-quakes. Soil Dyn Earthq Eng 26:115–130
Idriss IM, Boulanger RW (2010) SPT-based liquefaction triggering procedures. Report No. UCD/CGM-10-02. Center for Geotechnical Modeling, Department of Civil and Environmental Engineering, University of California, Davis
ISO 22476-1:2012 (2012) Geotechnical investigation and testing—field testing—part 1: electrical cone and piezocone penetration test
Iwasaki T, Tatsuoka F, Tokida K, Yasuda S (1978) A practical method for assessing soil liquefaction potential based on case studies at various sites in Japan. In: Proceedings of the 2nd international conference on microzonation. San Francisco, CA, USA, pp 885–896
Jorge C (1993) Zonation of liquefaction potential. Application attempt to the Portuguese Territory. M.Sc. in Sciences in Engineering Geology, New University of Lisbon
Jorge C, Vieira A (1997) Liquefaction potential assessment—application to the Portuguese Territory and to the Town of Setúbal. In: Sêco e Pinto (ed) Seismic behaviour of ground and geotechnical structures. Balkema, pp 33–43
Kayen R, Moss RES, Thompson EM, Seed RB, Cetin KO, Kiureghian A, Tanaka Y, Tokimatsu K (2013) Shear-wave velocity-based probabilistic and deterministic assessment of seismic soil liquefaction potential. J Geotech Geoenviron Eng 139(3):407–419. https://doi.org/10.1061/(ASCE)GT.1943-5606.0000743
LIQUEFACT (2017) Project overview. http://www.liquefact.eu. Accessed in November 2017
Marchetti S (1980) In situ tests by flat dilatometer. J Geotech Eng Div ASCE 106(GT3):299–321
Marchetti S (2016) Incorporating the Stress history parameter KD of DMT into the liquefaction correlations in clean uncemented sands. J Geotech Geoenviron Eng 142(2):04015072
Marchetti S, Monaco P, Totani G, Calabrese M (2001) The flat dilatometer test (DMT) in soil investigations—a report by the ISSMGE Committee TC16. In: Failmezger RA, Anderson JB (eds) Proceedings of international conference on insitu measurement of soil properties and case histories, Bali, 2001, official version reprinted in Flat Dilatometer Testing, Proceedings of 2nd international conference on the Flat Dilatometer, Washington D.C., April 2–5, 2006, pp 7–48

Marchetti S, Monaco P, Totani G, Marchetti D (2008) In situ tests by seismic dilatometer (SDMT). In: Laier JE, Crapps DK, Hussein MH (eds) From Research to Practice in Geotechnical Engineering, ASCE, Geotechnical Special Publication, vol 180, pp 292–311

Mayne PW (2006) In situ test calibrations for evaluating soil parameters. In: Proceedings of characterization and engineering properties of natural soils II, Singapore

Millen M, Ferreira C, Gerace A, Viana da Fonseca A (2019) Simplified equivalent soil profiles based on liquefaction performance. In: 7th international conference on earthquake geotechnical engineering. Rome, Italy

Monaco P, Marchetti S, Totani G, Calabrese M (2005) Sand liquefiability assessment by flat dilatometer test (DMT). In: Proceedings of the 16th international conference on soil mechanics and geotechnical engineering. Millpress Science Publishers/IOS Press, pp 2693–2697. https://doi.org/10.3233/978-1-61499-656-9-2693. Accessed 10 Jan 2019

Robertson PK (1990) Soil classification using cone penetration test. Canadian Geotech J 27:151–158

Robertson PK (2009) Interpretation of cone penetration tests: a unified approach. Can Geotech J 46(11):1337–1355

Robertson PK (2012) The James K. Mitchell Lecture: interpretation of in situ tests—some insights. In: Proceedings of 4th international conference on geotechnical and geophysical site characterization, Porto de Galinhas, vol 1, pp 3–24

Robertson PK, Wride CE (1997) Cyclic liquefaction and its evaluation based on SPT and CPT. In: Proceedings, NCEER workshop on evaluation of liquefaction resistance of soils

Rodrigues C, Amoroso S, Cruz N, Viana da Fonseca A (2016) Liquefaction assessment CPTu tests in a site in South of Portugal. In: Geotechnical and geophysical site characterisation 5—Lehane, Acosta-Martínezí, Kelly (eds). Australian Geomechanics Society, Sydney, Australia, pp 633–638. https://australiangeomechanics.org/wp-content/uploads/2017/02/ISC5_Proceedings-Vol1_20170209-ISBN-978-0-9946261-1-0-LowRes.pdf. Accessed 10 Jan 2019 (ISBN 978-0-9946261-2-7)

Saldanha AS, Viana da Fonseca A, Ferreira C (2018) Microzonation of the liquefaction susceptibility: case study in the lower Tagus valley. Geotecnia J Portuguese Geotech Soc 142:7–34. https://doi.org/10.24849/j.geot.2018.142.01

Seed HB, Idriss IM (1971) Simplified procedure for evaluating soil liquefaction potential. J Geotech Eng Div ASCE 97(9):1249–1273

Tonkin & Taylor (2013) Canterbury earthquakes 2010 and 2011. Land report as at 29 February 2012. Earthquake Commission, p 108. https://www.eqc.govt.nz/sites/public_files/documents/liquefaction-vulnerability-study-final.pdf. Accessed 10 Jan 2019

Viana da Fonseca A, Ferreira C, Ramos C (2017) D2.1—Part 2: report on ground characterization of the four areas selected as testing sites by using novel technique and advanced methodologies to perform in situ and laboratory tests—Lisbon Area in Portugal. Deliverable D2.1 of the European H2020 LIQUEFACT research project. January 2017

Viana da Fonseca A, Ferreira C, Saldanha AS, Ramos C, Rodrigues C (2018) Comparative analysis of liquefaction susceptibility assessment by CPTu and SPT tests. In: Hicks MA, Pisanò F, Peuchen J (eds) Cone penetration testing 2018, Proceedings of the 4th international symposium on cone penetration testing (CPT'18). CRC Press, Delft, pp 669–675

Wair BR, DeJong JT, Shantz T (2012) Guidelines for estimation of shear wave velocity profiles. PEER Report 2012/08. Pacific Earthquake Engineering Research Center

Wotherspoon LM, Orense RP, Green RA, Bradley BA, Cox BR, Wood CM (2015) Assessment of liquefaction evaluation procedures and severity index frameworks at Christchurch strong motion stations. Soil Dyn Earthq Eng 79(Part B):335–346. https://doi.org/10.1016/j.soildyn.2015.03.022

Affiliations

Cristiana Ferreira[1] · **António Viana da Fonseca**[1] · **Catarina Ramos**[1] · **Ana Sofia Saldanha**[2] · **Sara Amoroso**[3,4] · **Carlos Rodrigues**[5]

[1] CONSTRUCT-GEO, Faculty of Engineering of University of Porto, Rua Roberto Frias, s/n, 4200-465 Porto, Portugal

[2] Faculty of Engineering of University of Porto, Rua Roberto Frias, s/n, 4200-465 Porto, Portugal

[3] University of Chieti-Pescara, Viale Pindaro, Pescara, Italy

[4] Istituto Nazionale di Geofisica e Vulcanologia, Viale Crispi, L'Aquila, Italy

[5] Polytechnic Institute of Guarda, Av. Dr. Francisco Sá Carneiro, 50, 6300-559 Guarda, Portugal